International Journal of Innovative
Computing, Information and Control
Volume 16, Number 3, June 2020

ICIC International ©2020 ISSN 1349-4198
pp. 991–1006

THREE-DIMENSIONAL UAV COOPERATIVE PATH PLANNING BASED ON THE MP-CGWO ALGORITHM

Liuqing Yang[1,2], Jin Guo[3] and Yanbin Liu[4]

[1]Research Institute of Pilotless Aircraft
[2]Key Laboratory of Unmanned Aerial Vehicle Technology of Ministry of Industry and Information Technology
[3]College of Automation Engineering
[4]College of Astronautics
Nanjing University of Aeronautics and Astronautics
No. 29, Yudao Road, Qinhuai District, Nanjing 210016, P. R. China
{ yangliuqing; liuyb }@nuaa.edu.cn; 1851809251@163.com

Received August 2019; revised December 2019

Abstract. *A path planning method based on multi-population chaotic gray wolf optimization (GWO) is proposed to address the three-dimensional path planning problems that occur in multi-UAV cooperative task execution. First, on the basis of three-dimensional planning space, the cost function model of multi-UAV cooperation is established in accordance with the requirement of path planning. Moreover, an initial track set is constructed by combining with the multi-population concept. Second, given that the GWO algorithm is easy to fall into a local optimum, a chaotic search strategy is adopted to improve this algorithm. Finally, the proposed algorithm is used to solve the path planning problem of obtaining multiple cooperative paths. Simulation result shows that this algorithm can satisfy the constraints related to path planning and realize multi-UAV cooperative path planning. In comparison with GWO, EA, and PSO algorithms, stability and search accuracy are improved through the proposed algorithm.*

Keywords: Multi-UAV cooperation, Path planning, Gray wolf optimization, Multi-population, Chaotic local search

1. **Introduction.** In modern warfare, single UAV cannot satisfy the requirements of diversified operations given the limitation of operation scope and their functions. Multi-UAV cooperative operation has become a trend of future air battle because it can perform various operational tasks and effectively improve battle effectiveness. Therefore, lots of research have focused on the cooperative technologies of multiple UAV, such as mission planning [1], wireless sensor network [2] and formation control [3]. Multi-UAV cooperative path planning is one of key technologies of multi-UAV cooperative operation. At present, the methods for multi-UAV cooperative path planning are divided into two categories. One category includes methods developed from single UAV path planning, such as Voronoi diagram [4] and potential field [5]; another category refers to intelligent optimization algorithms, such as genetic algorithm [6], particle swarm optimization [7, 8], and ant colony algorithm [9, 10]. We can rapidly search many paths in a two-dimensional space using the first category to realize multi-UAV path planning. However, when the planning space is complex and the dimension increases, the computational and spatial complexities of the abovementioned methods increase. In recent years, swarm intelligent optimization algorithm has exhibited many advantages, such as strong search ability, favorable robustness, and easy to combine with other algorithms; thus, this algorithm has been applied

DOI: 10.24507/ijicic.16.03.991

to 2 or 3 dimension path planning of UAV, and has shown good performance in solving such complex optimization problems [11].

In 2014, Mirjalili et al. proposed a new simulated intelligent optimization algorithm called gray wolf optimization (GWO) [12]. This algorithm has a simple structure and a few adjusting parameters and is unrestricted by spatial structure. It has been proved that it is better than other optimization algorithms such as differential evolution (DE), particle swarm optimization (PSO) in terms of convergence speed and stability. Therefore, GWO has been extensively used in optimization. In path planning field, [13] demonstrates the application of this algorithm to path planning for UAV to achieve the optimal path search under different threat environments. In terms of path planning in a complex terrain environment, [14] conducts coefficient optimization through the GWO algorithm based on improved perturbation fluid algorithm for path planning and obtains a flying path that can avoid obstacles effectively and smoothly through a simulation experiment. In terms of UAV path planning in uncertain environment, [15] searches the optimal path through the GWO algorithm in Bayes framework model and confirms the effectiveness of this algorithm. However, these works only solve the route planning and obstacle avoidance problems of single UAV based on GWO, but have not use it for multi-UAV collaborative route planning. [16] extends GWO for 3D path planning of multiple UAV, and compares the performance with that of other meta-heuristic algorithms as well as deterministic algorithms. The results show that GWO algorithm outperforms the other algorithms in searching 3D path for multi-UAV. However, this approach did not solve the problem that the original GWO algorithm is easy to fall into the local optimization, and the time constraint problem in the actual task execution of UAV group is not been considered. In [17], GWO algorithm and Gaussian distribution estimation are combined to overcome the premature convergence of the original GWO algorithm, and the improved algorithm is applied to the path tracking of multiple UAV in urban environment. The experimental results demonstrated that the method performs well in accuracy and efficiency, but the complexity of this methods needs more computational cost.

In the present work, a multi-population chaotic GWO (MP-CGWO) is proposed to solve the problem on path planning when multi-UAV performs a cooperative strike on the known target. First, a track set is constructed by combining the idea of multi-population, and a chaotic local search is used to improve the problem in which the GWO algorithm easily falls into local optimization. Second, the improved method in the present work is adopted to solve the multi-UAV cooperative path planning problem, and a three-dimensional cooperative path that satisfies the planning requirements is obtained. Finally, a simulation experiment is conducted. The result is compared with DE, PSO, and GWO algorithms to verify the effectiveness of the proposed method.

2. **Modeling the UAV Cooperative Path Planning.** In this section, an appropriate planning space is established in accordance with the flight environment and mission requirements. And on the basis of planning space, we established a path cost function in accordance with the requirement of multi-UAV's path planning as an index to evaluate the quality of path.

2.1. **Planning space representation.** In path planning, an appropriate planning space must be established in accordance with the flight environment and mission requirements. In the present work, taking a mountain background as a task environment, a digital elevation model is established using a random function to simulate peaks and other threat obstacles. The mountain model function is proposed in [18]. This model consists of the original digital and threat equivalent terrain models. The former is expressed as

$$z_1(x,y) = \sin(y+a) + b\cdot\sin(x) + c\cdot\cos\left(d\cdot\sqrt{x^2+y^2}\right) + e\cdot\cos(y) + f\cdot\sin\left(f\cdot\sqrt{x^2+y^2}\right) + g\cdot\cos(y), \tag{1}$$

where x and y refer to the point coordinates on a horizontal projection plane; z_1 refers to the height coordinate that corresponds to the coordinate points on a horizontal plane; a, b, c, d, e, f and g are the coefficients. The topography of a different landform can be obtained by changing parameters.

The threat equivalent terrain model is

$$z_2(x,y) = \sum_{i=1}^{k} h(i)\cdot\exp\left(-\left(\frac{x-x_{0i}}{x_{si}}\right)^2 - \left(\frac{y-y_{0i}}{y_{si}}\right)^2\right), \tag{2}$$

where x and y refer to the point coordinates on a horizontal projection plane; z_2 refers to the height of the peak; $h(i)$ refers to the height of the highest point of Peak i on a base terrain; x_{0i} and y_{0i} refer to the coordinates of the highest point of Peak i; x_{si} and y_{si} refer to the variables related to the slope of peak i along the x, y axes. If x_{si} and y_{si} are large, then the slope of the peak is flat and abrupt.

The final mountain threat model is obtained by integrating the original digital terrain model into the threat equivalent terrain model.

$$z(x,y) = \max\left[z_1(x,y), z_2(x,y)\right]. \tag{3}$$

The topography of different landforms can be obtained by changing parameters in the function. The three-dimensional planning space is illustrated in Figure 1. In the planning space, the flying path of UAVs can be represented by many waypoint. Consequently, the waypoints are connected to form multiple flight paths, which are linked with the starting and target points to form a flying path. We set the starting point of a certain UAV as $\mathbf{S}(x_0, y_0, z_0)$ and the target point as $\mathbf{E}(x_e, y_e, z_e)$. The number of waypoints is n, and the waypoints searched can be represented by $\{\mathbf{S}, \mathbf{P}_1, \mathbf{P}_2, \ldots, \mathbf{P}_n, \mathbf{E}\}$; among these variables, the coordinate of a track node is $P_i = (x_i, y_i, z_i)$.

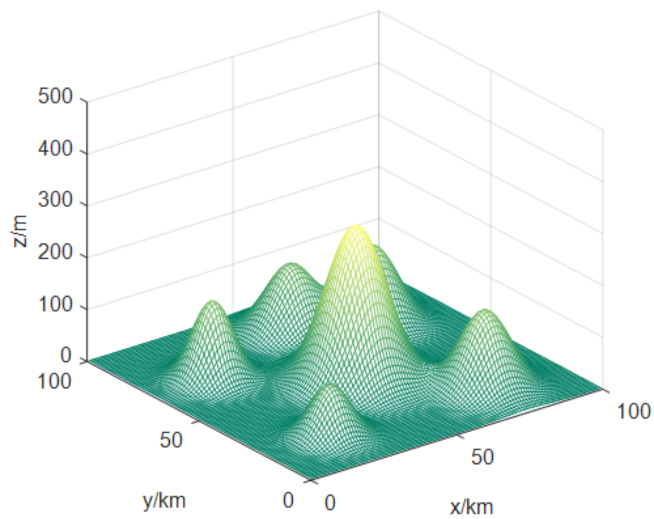

Figure 1. Three-dimensional planning space

2.2. **Path cost function.** The purpose of multi-UAV cooperative path planning is that, on the premise of satisfying the requirements of a safe flight and space-time cooperation, every UAV can search the corresponding path, and the synthetic path cost of UAV fleet must be the least. Therefore, path planning requires the establishment of a path cost function as an index to evaluate the quality of a path. The satisfaction of the spatial and temporal cooperative constraints of multi-UAV by considering the dynamics and threat constraints of a single UAV in multi-UAV cooperative path planning is required. Thus, given the planning objective, the following cost indexes are considered in the present work: the performance indexes of a single UAV include fuel consumption, maximum climb/slide angle, flying altitude, peak threat, and multi-UAV time cooperation. Spatial cooperation is manifested in multi-UAV path collision avoidance. We set different flight altitudes that must be avoided by each UAV. The synthetic cost function is established as

$$J = w_1 k_1 J_{fuel} + w_2 k_2 J_{angle} + w_3 k_3 J_{height} + w_4 k_4 J_{threat} + w_5 k_5 J_{coop}, \tag{4}$$

where w_1, w_2, w_3, w_4 and w_5 refer to the weights of different cost indexes, and the sum of weights is 1. The paths that satisfy different requirements can be obtained by adjusting the weights. To ensure that all cost indexes are involved in path planning, the functions are normalized in accordance with the range of their values, and then weighted summation is performed.

Fuel consumption cost is related to the length of flight path and flying speed. Assuming that UAVs consistently fly at a certain speed, fuel costs can be replaced by the length of the path.

$$J_{fuel} = \sum_{i=1}^{n-1} \sqrt{(x_{i+1} - x_i)^2 + (y_{i+1} - y_i)^2 + (z_{i+1} - z_i)^2}, \tag{5}$$

where $(x_{i+1}, y_{i+1}, z_{i+1})$ and (x_i, y_i, z_i) correspond to the coordinates of the adjacent path points.

J_{angle} refers to the cost of the maximum climb/slide angle and is expressed as

$$J_{angle} = \sum_{i=1}^{n} \theta_i \quad \theta_i = \arctan\left(\frac{|z_{i+1} - z_i|}{\sqrt{(x_{i+1} - x_i)^2 + (y_{i+1} - y_i)^2}}\right), \tag{6}$$

where θ_i refers to the climb/slide angle of the adjacent points of a certain path.

To satisfy the requirements of flight safety and concealment, the flight altitude cannot be overly low or high. Height cost can be expressed as

$$J_{height} = \sum_{i=1}^{n} |h_i - safth_i|, \tag{7}$$

where h_i refers to the height of path point i on a certain path, and $safth_i$ refers to the minimum safety height for each UAV.

Collision with the mountain in the flying course of the UAV must be avoided. In [19], the peak model is represented by a cone approximate representation. To ensure that the path between two waypoints can avoid the mountain, the path segment is divided into m equal sections, and $m - 1$ sampling points are obtained in the center. Since there is a certain error in approximating the mountain terrain as a cone, the flying height of the UAV is set higher than the current terrain height to ensure safe flight. The threat cost of the whole path is expressed as

$$J_{threat} = \sum_{i=1}^{n} \sum_{j=1}^{m} \sum_{k=1}^{K} threat_{ij}(k), \tag{8}$$

where n refers to the number of path points, K represents the number of peaks, and $threat_{ij}(k)$ is the threat cost of the sampling point (x_i, y_i, z_i) in the current section and a certain peak and is expressed as:

$$threat_{ij}(k) = \begin{cases} 0 & h_j > H(k) \text{ or } d_T > R_T + d_{T\min} \\ R_T(h) + d_{T\min} - d_T & h_j < H(k) \text{ and } d_T < R_T + d_{T\min} \end{cases}, \tag{9}$$

$$R_T(h) = (H(k) - h)/\tan\theta, \tag{10}$$

$H(k)$ refers to the height of Peak k, and R_T refers to the maximum extension radius. Moreover, h_j is the flying altitude of the current UAV, d_T refers to the distance from the UAV to the symmetrical axis of the peak, $d_{T\min}$ denotes the minimum distance allowed on the terrain, and θ refers to the slope of the terrain. The terrain threat is depicted in Figure 2.

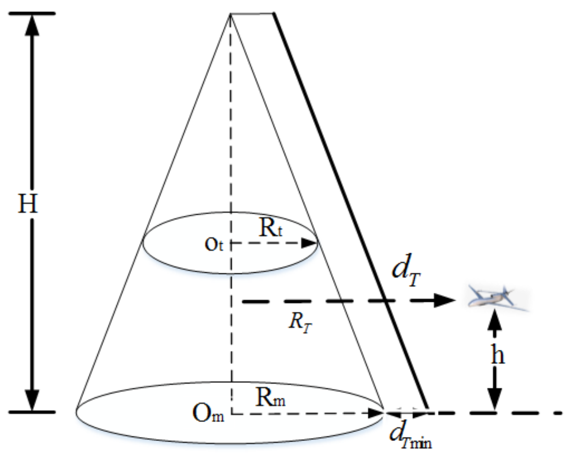

FIGURE 2. Terrain threat map

Cooperative cost function implies time cooperation. All UAVs are required to reach the target point simultaneously as far as possible. If the course of a certain path cannot satisfy the time cooperative constraints, then the path must be corrected. Assuming that the flying speed of the UAV is in the range of $[v_{\min}, v_{\max}]$ and the course of the UAV i is L_i, its flight time period is $T_i \in [T^i_{\min}, T^i_{\max}]$. Similarly, assuming that the flying time of UAV j is in the range of $T_j \in \left[T^j_{\min}, T^j_{\max}\right]$, if the flight time of the two UAVs intersects, then temporal cooperation is feasible, that is,

$$T_{inter} = T_i \cap T_j \neq \emptyset. \tag{11}$$

We set the length ratio of the intersection interval of two UAVs flight time periods to the smaller time period of the two time periods is not less than θ, that is $T_{inter} > \theta \cdot T_{\min}$, where $0 < \theta \leq 1$. According to the range of flight time intersection, the time synergy evaluation function between the routes is determined as follows:

$$J_{copT} = \begin{cases} 1 & T_{inter} = \emptyset \\ \dfrac{T_{inter}}{T_{\min}} & 0 < T_{inter} \leq \theta \cdot T_{\min} \\ 0 & T_{inter} > \theta \cdot T_{\min} \end{cases}, \tag{12}$$

where $T_{\min}$ refers to a time period with a small range of two path in the flight time period, and T_{inter} represents the intersection of the flight time for two paths.

3. **Solution of the Cooperative Path Planning Model Based on MP-CGWO.** In this section, a path planning method based on multi-population chaotic gray wolf optimization (GWO) is proposed to address the path planning problems of multi-UAV cooperative task execution.

3.1. **Introduction of the GWO algorithm.** The GWO algorithm is a new meta-heuristic algorithm based on the life habits of the gray wolf population. GWO has many advantages, such as simple structure, few parameters, and rapid convergence speed. In the algorithm, the ranking system of the gray wolf population in nature is simulated. The first three optimal individuals in the population are denoted as α, β, δ, and the remaining individuals are regarded as ω to determine the optimal solution that corresponds to the location of the prey. In searching for preys, each gray wolf obeys the instructions of the first three wolves, constantly updates their position, gradually approaches the most promising area (the optimal position), and catches the food. In the algorithm, the distance from the individuals to the prey must be determined.

$$D = \left| C \cdot \mathbf{X}_p(t) - \mathbf{X}(t) \right|, \tag{13}$$

$$C = 2 \cdot r_1, \tag{14}$$

where t refers to the number of current iterations, r_1 denotes a random value in the range of $[0, 1]$ and $\mathbf{X}$ represents the position vector of the gray wolf in Iteration t.

The gray wolf gradually approaches its prey and updates its position. The update is expressed as

$$\mathbf{X}(t+1) = \mathbf{X}(t) - A \cdot D, \tag{15}$$

$$A = 2a \cdot r_2 - a, \tag{16}$$

where a reduces from 2 to 0 gradually; r_2 refers to a random value in the range of $[0, 1]$.

The first three wolves represent historically optimal locations, while the remaining individuals update their locations in accordance with their present locations. Based on the abovementioned two formulas, the distance between the remaining individuals and the first three wolves, as well as the direction to the prey, can be obtained.

$$\begin{cases} D_\alpha = \left| C_1 \cdot \mathbf{X}_\alpha - \mathbf{X} \right| \\ D_\beta = \left| C_2 \cdot \mathbf{X}_\beta - \mathbf{X} \right| \\ D_\delta = \left| C_3 \cdot \mathbf{X}_\delta - \mathbf{X} \right| \end{cases}, \tag{17}$$

$$\begin{cases} \mathbf{X}_1 = \mathbf{X}_\alpha - A_1 \cdot D_\alpha \\ \mathbf{X}_2 = \mathbf{X}_\beta - A_2 \cdot D_\beta \\ \mathbf{X}_3 = \mathbf{X}_\delta - A_3 \cdot D_\delta \end{cases}, \tag{18}$$

$$\mathbf{X}(t+1) = \frac{\mathbf{X}_1 + \mathbf{X}_2 + \mathbf{X}_3}{3}, \tag{19}$$

where $\mathbf{X}_\alpha$, $\mathbf{X}_\beta$, $\mathbf{X}_\delta$ represent the positions of α, β, δ wolves, respectively. $\mathbf{X}$ denotes the location of the current solution.

3.2. **Algorithm improvement.**

3.2.1. *Multi-population track coding.* The original GWO algorithm is relatively small and has poor development ability in multi-UAV path planning. Therefore, on the basis of the original algorithm, the idea of multi-population is combined in this work to construct the multi-UAV track set. When the algorithm is adopted to perform a search, the number of gray wolf populations is determined in accordance with the number of UAVs, and the process of UAV searching path is mapped to the preying process of the gray wolf population. The position of the gray wolf in each sub-population corresponds to a flying path of the mapped UAV. The optimal solution in the sub-population corresponds to the optimal path of this UAV. The optimal solution of all sub-populations corresponds to the cooperative path of UAVs.

If all UAVs on a mission are set as $U = \{U_i, i = 1, 2, \ldots, N_u\}$, then the corresponding number of gray wolf population is N_u. The number of gray wolf individuals in each sub-population is set as m, and the gray wolf individuals in the sub-population can be represented as $\mathbf{X} = \{\mathbf{X}_i, i = 1, 2, \ldots, m\}$. The position of gray wolf i in the search space is $\mathbf{X}_i = (\mathbf{X}_{i1}, \mathbf{X}_{i2}, \ldots, \mathbf{X}_{in})$, which represents the midway point of a path in addition to the starting and the target points. The coordinate of each path point is $\mathbf{X}_{in} = (x_{in}, y_{in}, z_{in})$. The fitness value of the gray wolf individual corresponds to the cost function value of a certain path. If the fitness is favorable, then the path is optimal. In the process of searching and comparing the fitness values of individuals in the population, the gray wolf individuals at the favorable position are obtained as the α, β, δ wolves. The algorithm is guided to search continuously in the direction with small fitness values, thereby resulting in many cooperative paths.

When the GWO algorithm is initialized, a group of gray wolves is randomly generated in the region of search. When an individual's three-dimensional position coordinates are randomly generated, the computational load is large, and the search efficiency is low. Therefore, in this work, an equal division is performed for the coordinates of individuals in the direction of the x-axis based on the number of the waypoints set at initialization. In the searching process, the positions in the y- and z-axes are updated. Boundary control is performed when the position is updated. The planning problem is transformed into a search optimization problem in a two-dimensional space.

3.2.2. *CGWO algorithm.* The GWO algorithm has few parameters, simple structure, and fast convergence speed. However, similar to other intelligent optimization algorithms, the GWO algorithm can easily fall into the local optimum problem, whereby the path searched is not necessarily optimal in path planning. To improve the quality of the search path, we consider adding a chaotic local search (CLS) strategy based on the GWO algorithm. Therefore, the randomness and ergodicity of a chaotic motion can be utilized to prevent the GWO algorithm from falling into the local optimum and thus improve convergence accuracy.

Chaotic motion is a common phenomenon in nonlinear dynamic systems with randomness, ergodicity, boundedness, and other characteristics. These characteristics help the optimization algorithm jump out of local extremum. The dynamic characteristics of the chaotic motion can optimize the algorithm to explore additional search space and improve the ability of global optimization. At present, many kinds of chaotic maps have been applied to optimization algorithms [20]. Logistic mapping is a typical one-dimensional chaotic mapping, and its analytic expression is

$$x_{n+1} = \mu x_n \left(1 - x_n\right), \tag{20}$$

where μ refers to a control parameter, and the initial value $x_0 \in [0, 1]$. Different chaotic sequence diagrams can be obtained by different x_0 and μ. When μ is 4, the chaotic motion is in a completely chaotic state. The chaotic sequence searches all states in the interval of $[0, 1]$ without any repetition. Thus, a local search can be performed near the search point using the characteristics of the chaotic motion. This process can effectively make the original algorithm jump out of the local optimum. The process for improving the GWO algorithm using the chaotic local search is presented as follows.

1) Chaotic initialization population

Determine the search boundary $[lb, ub]$ in accordance with the planning space. Given the number of path points set as m-dimension, 2N m-dimension in the chaotic sequence in the interval of $[0, 1]$ is generated using a logistic equation. In accordance with the searching boundary, the equation is mapped on the planning space.

Calculate the fitness values of the 2N individuals. The first N individuals with favorable fitness are selected as the initial gray wolf population for a path search.

2) Local chaotic search

Obtain a new gray wolf individual $\mathbf{X}_c$ by generating the n-dimensional chaotic random sequence z: $x_0, x_1, \ldots, x_n$ in the interval of $[0, 1]$ through K iterations using a logistic equation and mapping the equation on the area near the path search point using Formula (21).

$$\mathbf{z} \to \mathbf{X}_c : \mathbf{X}_c = \mathbf{X}_\alpha + R \cdot (\mathbf{z} - 0.5), \tag{21}$$

where R refers to the search radius, which can be used in controlling a local search range, and $\mathbf{X}_\alpha$ refers to the position of α wolf.

Calculate the fitness value of $\mathbf{X}_c$. Compare the new individual with the optimal individual $\mathbf{X}_\alpha$ under the current iteration times through the GWO algorithm. If the fitness value is less than that of the original individual, then the new individual is used to replace the original individual; otherwise, the original individual will remain unchanged.

When the improved chaotic GWO algorithm is used for path planning, the fitness value of individuals in the population corresponds to the path cost value of UAV. The chaotic strategy is for individual initialization and updating the position of the optimal individual in the iteration process. The improved GWO algorithm is as follows.

Algorithm 1
CGWO algorithm

```
Begin
    Initialize chaotic grey wolf population;
    Initialize parameters a, A, C by (14) and (16);
    For all X_i wolfs do
        Calculate fitness by (4);
    End for
    Get the first three individuals as X_α, X_β, X_δ;
    While t < Maximal number of iterations do
        For Each search wolf do
            Update the position of the wolf by (19)
        End for
        Update a, A, C;
        Calculate fitness of all search wolves and identify the best individual X_α;
        Implement chaotic local search around X_α, and update X_α;
        t = t + 1;
    End while
    Return X_α;
End
```

3.3. **Flow of the multi-UAV cooperative path planning.** Each UAV has a corresponding starting point and target point, and the flight time to perform mission depends on path length and flight speed. Defining the flight speed of the drone as $v_i \in [v_{i\min}, v_{i\max}]$, $v_{i\min}$ and $v_{i\max}$ correspond to the minimum flight speed and the maximum flight speed respectively. By adjusting the speed of UAV, the UAV group can meet the time coordination requirement. When planning with this algorithm, the number of sub-populations is determined according to the number of UAV, the position of gray wolf in each sub-population corresponds to a flying path of the mapped UAV. And each sub-group searches the flight path of the corresponding UAV, the optimal solution $\mathbf{X}_\alpha$ in the sub-population corresponds to the optimal path of this UAV.

During the search process, the fitness value of the individual in the population is determined by the route cost which can be calculated by (4). The smaller the cost of the route, the smaller the fitness value of the gray wolf in the position $\mathbf{X}_i$, which means the route is better. As the number of iterations increases, individuals in the population continually converge toward the position of the optimal track according to the social hierarchy and the position update rule, i.e., (19), and finally we can obtain the optimal search results of all sub-populations corresponding to the cooperative path of UAVs, and then output the search results, that is, the cooperative route.

Based on the improved algorithm in this work, the specific step of the multi-UAV cooperative path planning is represented in Algorithm 2. And the flow of the path planning of multiple UAV is shown in Figure 3.

Algorithm 2
MP-CGWO algorithm for multi-UAV cooperative path planning

```
Begin
    Initialize parameters: number of populations, max iterations, dimension (number of waypoints);
    For all UAV_i do
      Initialize subpopulation position of multi-UAV;
      Initialize parameters a, A, C by (14) and (16);
      For all X_i do
          Calculate the weighted sum of path cost J by (4);
      End for
      Get the first three paths as X_α, X_β, X_δ;
      While t < Maximal number of iterations do
          For Each search path do
            Update the position of UAV by (19);
          End for
            Update a, A, C;
            Calculate the weighted sum of path cost J by (4) and identify the best path X_α;
            Implement chaotic local search around X_α, and update X_α;
            t = t + 1;
      End while
     End for
     Output the paths;
End
```

4. **Simulation Validation.** In this section, we perform two simulation cases to verify the effectiveness and performance of the proposed algorithm. Moreover, in order to determine whether the results of the method differ from the best results of other algorithms, a comparative validation is conducted.

4.1. **Simulation environment setting and simulation analysis.** The planning space is set as 100 km $\times$ 100 km $\times$ 500 m, including six peaks, and the mountain threat model can be established according to Formula (3). At the same time, we can get different

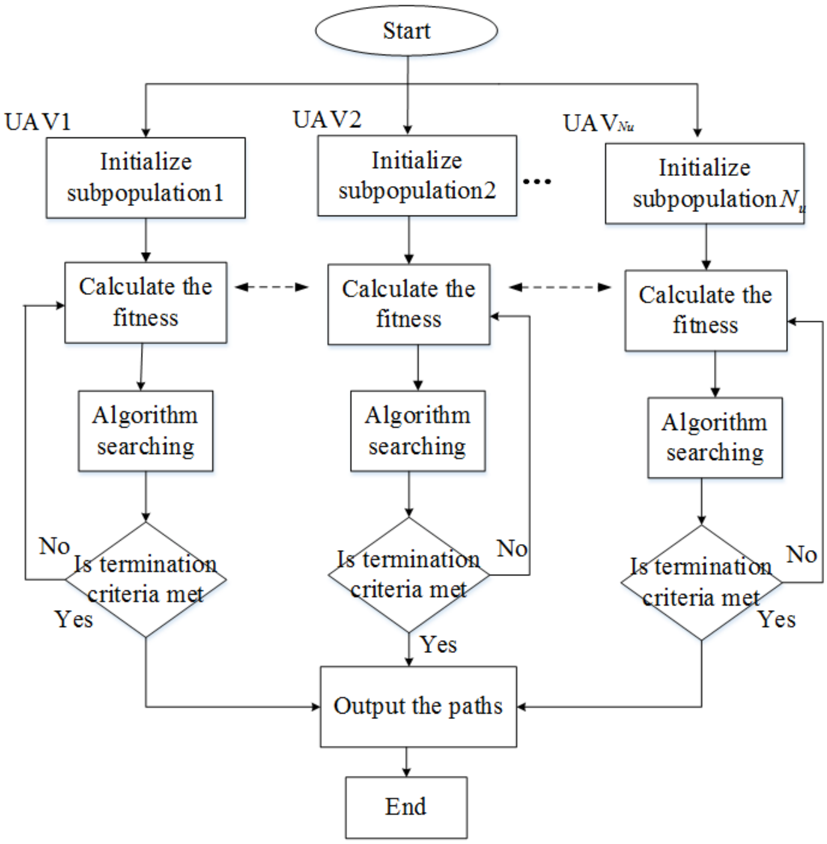

FIGURE 3. Flowchart of path planning of multiple UAV

TABLE 1. Peak model parameters

Number	Height (m)	Center location $(x, y)/(\text{km})$	Slope
1	130	$(56, 82)$	$(10, 10)$
2	150	$(75, 20)$	$(10, 10)$
3	300	$(50, 45)$	$(12, 12)$
4	100	$(22, 20)$	$(8, 8)$
5	150	$(20, 70)$	$(8, 8)$
6	150	$(75, 75)$	$(10, 10)$

topography by setting different parameters. Referring to [21], the parameters of the original digital terrain model are set to $a = 0.1$, $b = 0.01$, $c = 1$, $d = 0.1$, $e = 0.2$, $f = 0.4$, and $g = 0.02$. The height of the peak, horizontal coordinates of the highest point, and slope parameters are listed in Table 1. Multi-UAV cooperative path planning is conducted under a known mission assignment scheme. In the simulation experiment, the path sub-population is initialized in accordance with the number of UAVs. The numbers of individuals in the sub-population, iterations, and path points are 20, 150, and 10, respectively. The weight coefficients of all cost functions correspond to 0.3, 0.2, 0.1, 0.2, and 0.2. The flight speed range of the UAV is 40-60 m/s.

Case 1: 3 UAVs begin from the starting point and arrive at the designated target point to perform tasks. The coordinates of the starting and target points are presented in Table 2. To verify the effectiveness of this method and avoid the influence of randomness, 50 simulation operations are established. The three-dimensional path planning and contour

Table 2. Coordinates of the starting and target points of all UAVs

Number	Start point	Target point
UAV1	$(3, 3, 0)$	$(95, 10, 70)$
UAV2	$(15, 1, 0)$	$(98, 92, 70)$
UAV3	$(1, 15, 0)$	$(92, 98, 70)$

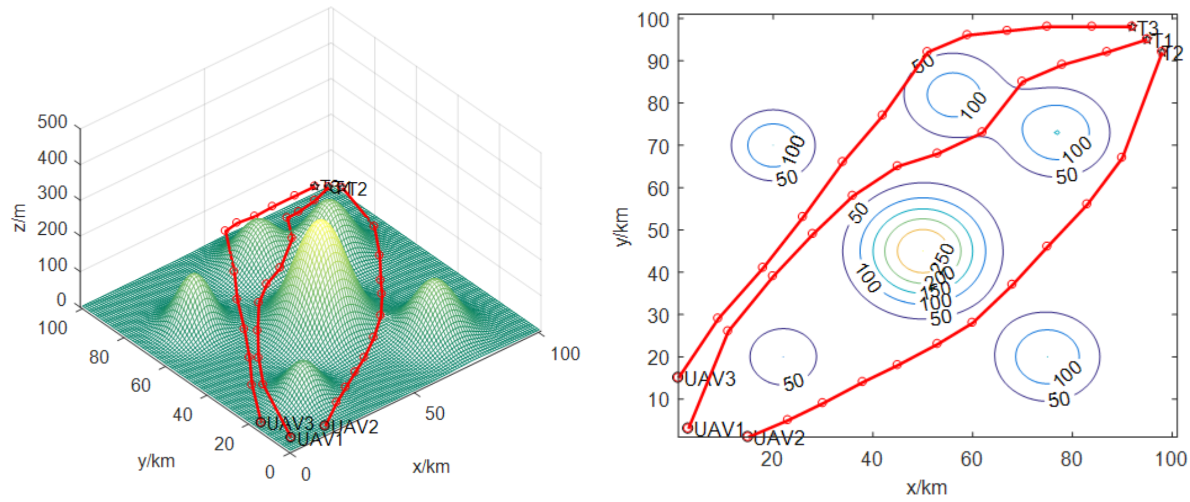

(a) Three-dimensional cooperative path map (b) Contour map

Figure 4. Three-dimensional cooperative path planning and contour map (Case 1)

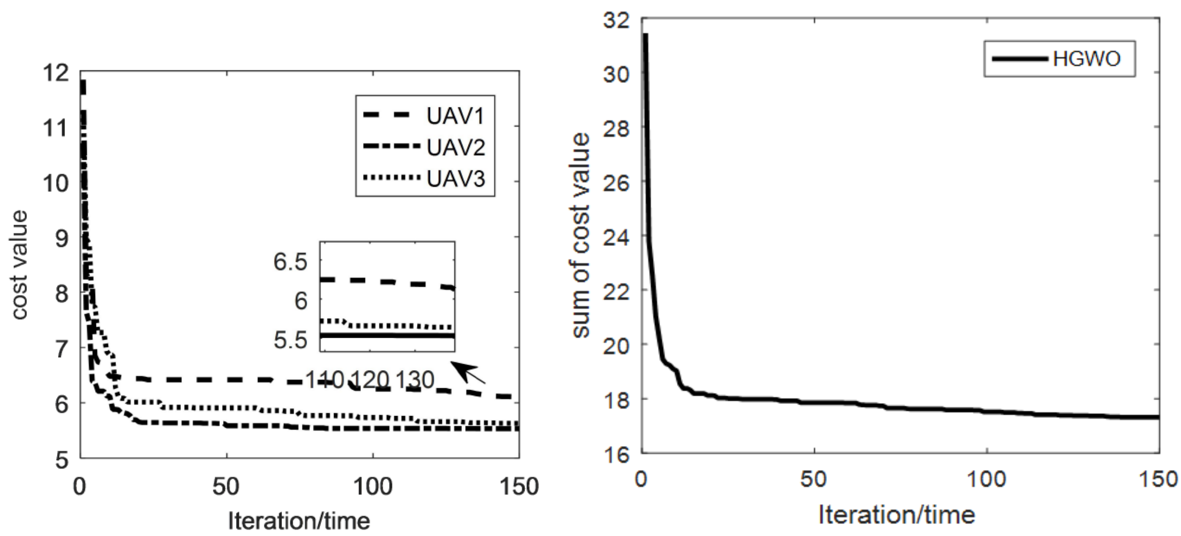

(a) (b)

Figure 5. Path cost convergence curve based on MP-CGWO (Case 1)

map of each UAV are displayed in Figures 4(a) and 4(b). The cost and synthetic path cost convergence curves of each UAV are plotted in Figures 5(a) and 5(b).

Figure 4 illustrates that all UAVs can effectively avoid the threat and reach the target points from their starting points, and the curves are smooth enough for UAV to fly. Figure

5(a) shows the path cost convergence curve of each UAV, as we can see, all curves can converge rapidly, in which the minimum route cost values of UAV1, UAV2 and UAV3 are respectively 6.25, 5.66, 5.54. Figure 5(b) shows the comprehensive route cost of UAV group, and it can be seen that this curve also rapidly converges to the optimal value. The cost function values of each UAV gradually converge with the increase in iteration times, thereby verifying the effectiveness of the algorithm. Through a simulation, the flight time intervals (unit: s) of each UAV are $[2315, 3473]$, $[2131, 3196]$, and $[2315, 3373]$. The time intersection is $[2315, 3196]$. The time synergy requirement can be satisfied by setting different flight speeds for all UAVs.

Case 2: Six UAVs fly to two target points. The coordinates of the starting and the target points are listed in Table 3.

TABLE 3. Coordinates of the starting and target points for all UAVs

Number	Start point	Target point
UAV1	$(1, 1, 0)$	$(95, 10, 70)$
UAV2	$(1, 20, 0)$	$(95, 10, 70)$
UAV3	$(1, 40, 0)$	$(95, 10, 70)$
UAV4	$(1, 60, 0)$	$(99, 75, 70)$
UAV5	$(1, 75, 0)$	$(99, 75, 70)$
UAV6	$(1, 95, 0)$	$(99, 75, 70)$

The planned path diagrams of UAVs are obtained after 50 simulations, as depicted in Figure 6. The path cost convergence and synthetic cost curves of each UAV are plotted in Figure 7. The planned paths and voyages are close and can effectively avoid obstacles. If the UAV is close to one another, then collisions can be avoided by setting different flight altitudes.

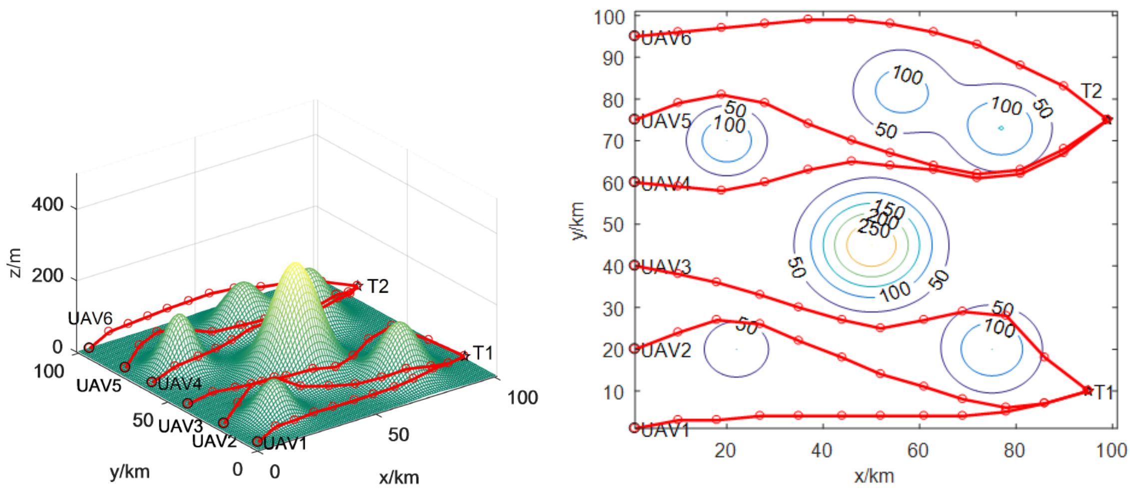

(a) Three-dimensional cooperative path map (b) Contour map

FIGURE 6. Three-dimensional cooperative path planning and contour map (Case 2)

From the 3D path map and contour map of Figure 6, it can be seen that all UAVs can reach the specified target point under the premise of ensuring their own safe flight. Meanwhile, the flight paths meet the requirements of obstacle avoidance, terrain avoidance and flight altitude. Figure 7(a) shows the convergence curve of the route cost for each

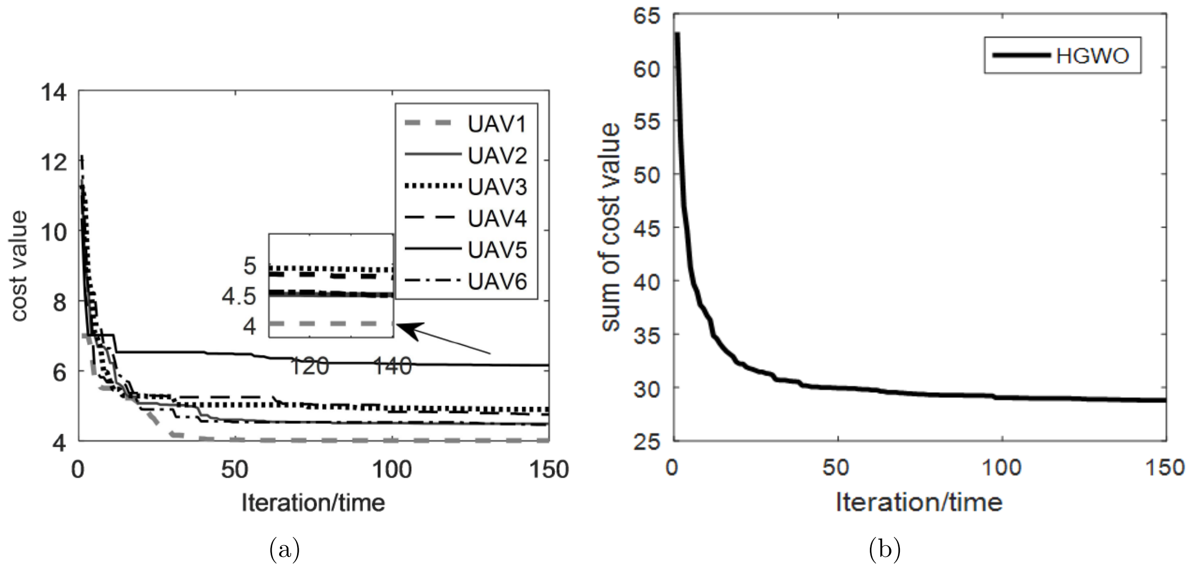

FIGURE 7. Path cost convergence curve based on MP-CGWO (Case 2)

UAV, and it can be seen that each curve can converge quickly. Because of the difference between the starting point and the target point of each UAV, the searched flight paths and path cost value are also somewhat different. Each UAV's minimum route value is respectively 4.02, 4.53, 4.90, 4.80, 6.16, 4.48. As seen from Figure 7(b), the integrated route cost also quickly converges to the optimal value. After simulation, we get the time intersection is $[2315, 3196]$ which satisfies time synergy requirement. From all simulation results we could conclude that the proposed algorithm can solve path planning problem of multiple UAV and obtain optimal paths for each UAV in the environment with obstacles.

4.2. **Comparative validation.** Based on Case 1, the PSO, DE, and GWO algorithms are used for multi-UAV cooperative path planning. The simulation results are compared with the proposed algorithm to verify the effectiveness of the improved strategy. Among these factors, the PSO algorithm parameters [22] include the number of particles as 20, learning factor $c1 = c2 = 1$, and inertia factor that decreases linearly from 0.96 to 0; the DE algorithm parameters [23] include the number of chromosomes as 20, the upper (0.6) and lower (0.2) bounds of scaling factor, and mutation rate (0.5) and crossover probability (0.85). The GWO algorithm is consistent with the improved algorithm. The algorithm is performed 50 times each. The average convergence curve after 150 iterations of each algorithm and the distribution of the minimum cost results after each iteration are obtained, as exhibited in Figures 8 and 9. The minimum, maximum, average, and standard deviation of the global optimum are summarized in Table 4.

Figure 8 displays that the cost function of each algorithm can converge to a certain value. By comparison, the convergence speed is faster in this method than that in other algorithms, and the convergence accuracy is better in this method than in the PSO algorithm and the original GWO algorithm. Figure 9 displays the distribution of the minimum path cost value in 50 simulations and the stability of these methods can be observed from the minimum cost distribution map. The minimum cost value obtained by this method is concentrated in the interval $[13.01, 13.47]$. Obviously, the interval range is significantly smaller than the other three algorithms. Simultaneously, Table 4 displays that the minimum path cost values of all algorithms in 50 simulations are basically the same. However, the average and variance are smaller in the MP-CGWO algorithm than in other algorithms. Compared with GWO algorithm, the stability (standard deviation)

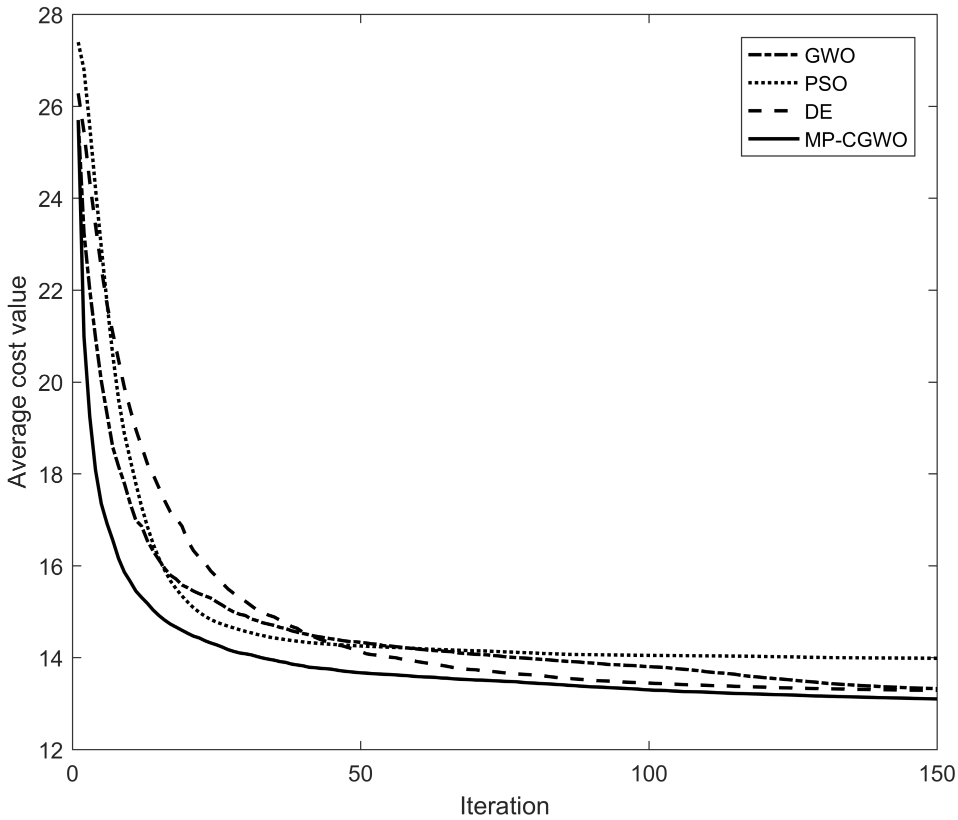

FIGURE 8. Average path cost convergence curve (50 times)

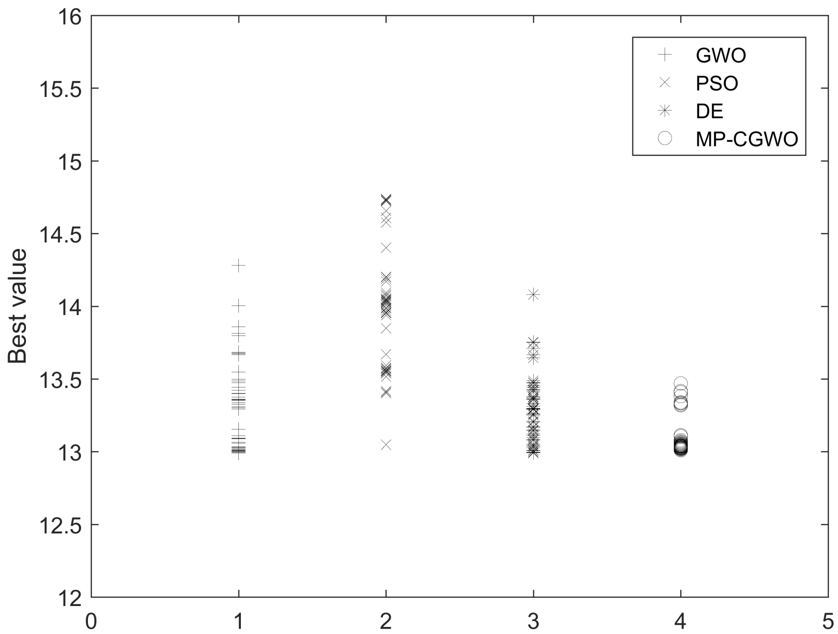

FIGURE 9. Distribution map of the minimum path cost value

of the MP-CGWO algorithm is improved by 56%, which means the effectiveness of the improved algorithm. Given that the chaotic mechanism is added to the algorithm, the algorithm can effectively jump out of the local optimum, and the ability of planning path is improved. The planning time of these approaches is close except for that of DE. Although

Table 4. Comparison of statistical results of algorithms (50 times)

Algorithm	Best cost	Worst cost	Mean	Std	Time/s
GWO	13.00	14.28	13.33	0.30	3.58
PSO	13.05	14.73	14.00	0.40	3.80
DE	13.00	14.08	13.29	0.24	5.99
MP-CGWO	13.01	13.47	13.10	0.13	3.88

the complexity of algorithm increases, the planning time does not change much compared to the original GWO and PSO, and remains less than the simulation time of the DE algorithm. Thus, the actual requirements for planning are satisfied. Overall, the capacity of path planning for multi-UAV of MP-CGWO is better than or at least competitive with the other algorithms, verifying the stability and effectiveness of MP-CGWO in the path search process.

5. Conclusions.

Based on the three-dimensional planning space, this work combines the idea of multi-population to perform multi-UAV cooperative path planning coding. Through chaotic local search, the disadvantage that the GWO algorithm can easily fall into the local optimum is addressed. The algorithm is adopted in studying the three-dimensional multi-UAV cooperative path planning. The simulation results show that the method can be used to obtain the cooperative path that satisfies the constraints. The comparison with three other algorithms verifies the effectiveness of the algorithm in solving cooperative path planning. In addition, search accuracy and stability are improved significantly. This work simplifies the multi-UAV collision avoidance constraints regardless of the change in the battlefield environment. In the next stage, we will explore the problem of multi-UAV cooperative path planning in a changing environment.

Acknowledgment. This work is partially supported by Nanjing Special Fund for Fundamental Research Business Expenses (NZ2018008). The authors also gratefully acknowledge the helpful comments and suggestions of the reviewers, which have improved the presentation.

REFERENCES

[1] Z. Y. Zhen, D. J. Xing and C. Xing, Cooperative search-attack mission planning for multi-UAV based on intelligent self-organized algorithm, *Aerospace Science and Technology*, vol.76, no.5, pp.402-411, 2018.

[2] M. A. Sayeed and R. Shree, Optimizing unmanned aerial vehicle assisted data collection in cluster based wireless sensor network, *ICIC Express Letters*, vol.13, no.5, pp.367-374, 2019.

[3] Y. Zou, Z. Q. Zhou, X. W. Dong et al., Distributed formation control for multiple vertical takeoff and landing UAVs with switching topologies, *IEEE/ASME Trans. Mechatronics*, vol.23, no.4, pp.1750-1761, 2018.

[4] P. B. Ma, Z. E. Fan and J. Jun, Cooperative control of multi-UAV with time constraint in the threat environment, *2014 IEEE Chinese Guidance, Navigation and Control Conference*, pp.2424-2428, 2014.

[5] O. Cetin, I. Zagli and G. Yilmaz, Establishing obstacle and collision free communication relay for UAVs with artificial potential fields, *Journal of Intelligent and Robotic Systems*, vol.69, nos.1-4, pp.361-372, 2013.

[6] E. Halit and L. Kemal, 3D path planning for multiple UAVs for maximum information collection, *Journal of Intelligent and Robotic Systems*, vol.73, nos.1-4, pp.737-762, 2014.

[7] K. A. Ghamry, M. A. Kamel and Y. M. Zhang, Multiple UAVs in forest fire fighting mission using particle swarm optimization, *2017 International Conference on Unmanned Aircraft Systems*, pp.1404-1409, 2017.

[8] Y. Liu, X. J. Zhang, Y. Zhang et al., Collision free 4D path planning for multiple UAVs based on spatial refined voting mechanism and PSO approach, *Chinese Journal of Aeronautics*, vol.32, no.6, pp.1504-1519, 2019.

[9] J. Dentler, M. Rosalie, G. Danoy et al., Collision avoidance effects on the mobility of a UAV swarm using chaotic ant colony with model predictive control, *Journal of Intelligent and Robotic Systems*, vol.93, nos.1-2, pp.227-243, 2019.

[10] P. C. Sara, B. P. Eva, A. O. Jose et al., Ant colony optimization for multi-UAV minimum time search in uncertain domains, *Applied Soft Computing Journal*, vol.62, no.1, pp.789-806, 2018.

[11] X. S. Yang, S. Deb, S. Fong et al., From swarm intelligence to metaheuristics: Nature-inspired optimization algorithms, *Computer*, vol.49, no.9, pp.52-59, 2016.

[12] S. Mirjalili, S. M. Mirjalili and A. Lewis, Grey wolf optimizer, *Advances in Engineering Software*, vol.69, no.3, pp.46-61, 2014.

[13] S. Zhang, Y. Q. Zhou, Z. M. Li et al., Grey wolf optimizer for unmanned combat aerial vehicle path planning, *Advances in Engineering Software*, vol.99, no.9, pp.121-136, 2016.

[14] P. Yao and H. L. Wang, Three-dimensional path planning for UAV based on improved interfered fluid dynamical system and grey wolf optimizer, *Control and Decision*, vol.31, no.4, pp.701-708, 2016.

[15] M. Radmanesh, M. Kumar and M. Saim, Grey wolf optimization based sense and avoid algorithm in a Bayesian framework for multiple UAV path planning in an uncertain environment, *Aerospace Science and Technology*, vol.77, no.6, pp.168-179, 2018.

[16] R. K. Dewangan, A. Shukla and W. Wilfred, Three dimensional path planning using grey wolf optimizer for UAVs, *Applied Intelligence*, vol.49, no.6, pp.2201-2217, 2019.

[17] X. F. Wang, H. Zhao, T. Han et al., A grey wolf optimizer using Gaussian estimation of distribution and its application in the multi-UAV multi-target urban tracking problem, *Applied Soft Computing Journal*, vol.78, pp.240-260, 2019.

[18] Z. Cheng, X. Y. Tang and Y. L. Liu, 3-D path planning for UAV based on chaos particle swarm optimization, *Applied Mechanics and Materials*, vol.232, pp.625-630, 2012.

[19] Z. H. Hu, *Research on Some Key Techniques of UAV Path Planning Based on Intelligent Optimization Algorithm*, Ph.D. Thesis, Nanjing University of Aeronautics and Astronautics, China, 2011.

[20] M. Kohli and S. Arora, Chaotic grey wolf optimization algorithm for constrained optimization problems, *Journal of Computational Design and Engineering*, vol.5, no.4, pp.458-472, 2018.

[21] D. Zhao and L. Qi, Three-dimensional route planning of UAV based on ACO-PSO algorithm, *Journal of Jilin Institute of Chemical Technology*, vol.34, no.3, pp.93-98, 2017.

[22] H. Y. Tang, S. R. Peng, J. J. Sun et al., 3D route planning of UAV based on SAPSO algorithm, *Tractical Missile Technology*, vol.2, pp.62-68, 2017.

[23] L. H. Wu, Y. N. Wang, X. F. Yuan et al., Differential evolution algorithm with adaptive second mutation, *Control and Decision*, vol.8, pp.898-902, 2006.